

Evaluation of the Surface Properties of Nanoparticles

Evaluation of the Surface Properties of Nanoparticles

A. Keller, K. Siegmann, and H.C. Siegmann

*Laboratory for Combustion Aerosols and Suspended Particles
Swiss Federal Institute of Technology (ETH)
CH-8093 Zürich, Switzerland*

Abstract - Most of the nanoparticle properties are governed by the chemical and physical nature of the surface. However, the relevant surface area is not the geometrical surface but only a fraction of it called the Active Surface. Experimentally, one obtains this A-Surface either from a measurement of the mobility b or equivalently from the mass transfer coefficient K . K has been determined either by attachment of radioactive Pb-atoms or simply by diffusion charging of neutralized particles. We show that $K \cdot b = \text{const}$ independent of particle material or shape. This empirical rule is useful for intercomparison and calibration of various instruments based on different physical principles. Dynamical changes of the A-surface can be observed by measuring the photoelectric yield of the particles while suspended in their proper carrier gas.

Introduction

In the macroworld, the surface of a body may change without affecting its physical and chemical properties nor its motion under the influence of a force. This changes dramatically as one moves to nanosized bodies suspended in a carrier gas. In this situation, the surface properties have the dominant influence on condensation of vapors, chemical reaction rates, and catalytic activity, as well as on particle deposition on a substrate by impaction or diffusion. This is crucial to the health effects induced by nanoparticles as they are deposited in the human respiratory tract. Even the determination of the "size" of the particle rests on the measurement of a surface property such as the mobility of the particle under the influence of an external force. It is the purpose of this paper to show how one can determine the relevant surface properties. It will also be demonstrated that only a fraction of the geometrical surface is active. This active surface determines both, the electrical mobility b and the mass transfer coefficient K from the gas phase to the particle. The concept of the active surface also leads to a simple empirical relation $K \cdot b = \text{const}$. This relation turns out to be valid independently of the shape of the particles and their chemical nature over a large range of nanoparticles in the difficult

transition between macroscopic and molecular particle motion. We will further show that photoelectric charging of the particles yields the active surface as well and allows one to observe its dynamical changes as the particle interacts with the carrier gas.

Theoretical background

The mobility b of a particle is defined by:

$$V = b \cdot F \quad (1)$$

where V is the velocity of the particle. The force F is generated by putting one elemental charge e on the particle and bringing it in an electric field E , $F = e \cdot E$. b is generated by the friction the particle experiences in the carrier gas.

For particles with a diameter $d_p \gg \lambda$ where λ is the mean free path of the gas molecules, the particle performs a hydrodynamic motion. ($\lambda=65$ nm for air at normal conditions). In the limit of small velocities V and for particles of spherical shape, the flow around the particle is laminar, and one finds according to Stokes that b is proportional to $1/d_p$.

The molecular particle motion occurs for $d_A \ll d_p \ll \lambda$ where d_A is the diameter of the gas molecules. The friction is then due to the difference in pressure generated by the reflection of gas molecules on the front and the backside of the particle. This leads to $b \propto 1/d_p^2$. There are some uncertain numerical factors due to the fact that one does not know whether the reflection of the gas molecules on the particle is specular or diffuse. The relevant surface related factor $1/4 \pi d_p^2$ is the cross section of the particle averaged over all directions as the particle performs a random Brownian rotation when it is dragged through the gas by the external force F .

The transition regime occurs at $d_p \approx \lambda$. There is no theory in this transition as laminar flow around a particle in vigorous Brownian motion makes no sense. However, one has agreed to assume a smooth transition between the molecular $b \propto 1/d_p^2$ and the macroscopic $b \propto 1/d_p$ regime according to the formula given by N.A. Fuchs¹. Yet one has to keep in mind that, due to the absence of a theory, d_p in the transition regime is only a parameter and no physical meaning may be attached to it.

The mass transfer coefficient K is defined by

$$dn/dt = -K \cdot N \cdot n \quad (2)$$

where N is the number density of the particles and n the density of the molecular species attaching themselves to the particle at the rate of dn/dt . K measures the growth rate of the particles by condensation of the species n .

In the macroscopic regime with $d_p \gg \lambda$, the molecules diffuse to the particles. This yields

$$K = 2\pi D d_p \quad (3)$$

D is the diffusion constant. It is assumed that once a particle hits the surface, it is not reflected but sticks to the particle. This is realistic only for electrically charged molecules or for very reactive radicals or atoms such as metal atoms. Other molecules like NO_2 or O_3 have sticking probabilities of the order of 10^{-4} , see Ref. 2.

In the molecular regime with $d_A \ll d_p \ll \lambda$, the molecules fly in vacuo near the particle. Whether or not they hit the particle again depends mainly on its cross section $1/4 \pi d_p^2$ averaged over all directions. This yields

$$K = (\pi/4) \cdot v d_p^2 \quad (4)$$

where v is the average thermal velocity of the carrier gas molecules.

In the transition regime, one has to take account of the fact that the adsorbing species first has to perform a classical diffusion to the neighborhood of the particle from where on the gas kinetics dominate. Following Filippov³ the last step is best treated in a Monte Carlo calculation of the actual pathways of the molecules. This has the advantage over the older approximations that gas collisions close to the particle are properly taken into account and that even complex interactions such as occurring between a charged molecule and the image charge induced in the particle can be accounted for in a realistic way. What it all amounts to is that once again a transition occurs from the macroscopic regime where $K \propto d_p$ to the molecular regime with $K \propto d_p^2$. Since the mobility b varies first with d_p^{-1} and then with d_p^{-2} , one might expect that

$$K \cdot b = \text{const} \quad (5)$$

This is not guaranteed however as the transition could occur at a different rate for the friction $1/b$ and the mass transfer K . Therefore, one needs experiments to decide on the validity of eq. (5) in the transition regime.

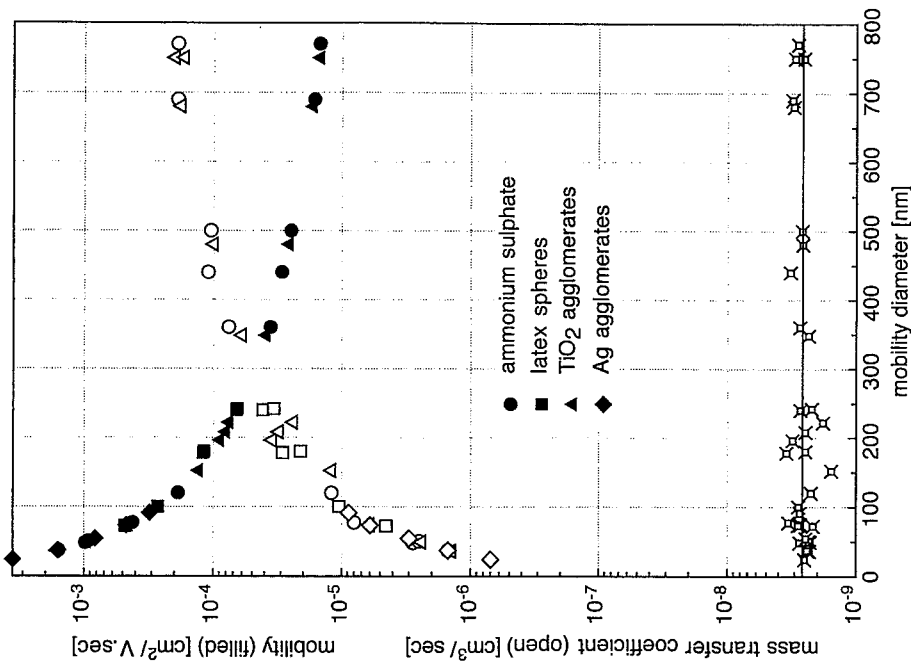


Figure 1. Electrical mobility b , mass transfer coefficient K and the product Kb vs. the mobility diameter for a variety of particles. K was measured by attachment of radioactive Pb . The data are adapted from Ref. 4 and Ref 9. The average value of $Kb = 2.616 \cdot 10^{-9} [\text{cm}^5/(\text{Vs}^2)]$

Experimental evidence for $K \cdot b = \text{const}$ and the concept of the Active Surface

Rogak, Baltensperger, and Flagan⁴ measured the electrical mobility b of titanium oxide particles and their agglomerates, of latex spheres, and of ammonium sulphate droplets over a wide range of particle sizes and shapes. They simultaneously determined the attachment rate of radioactive lead atoms and obtained the mass transfer coefficient K for each particle mobility. Fig. 1 shows their results for K and b plotted against the mobility diameter as calculated from b according to Fuchs¹. We see that indeed $K \cdot b = \text{const}$ over a large range of mobilities and that this is independent of the chemical composition of the particles within experimental uncertainty.

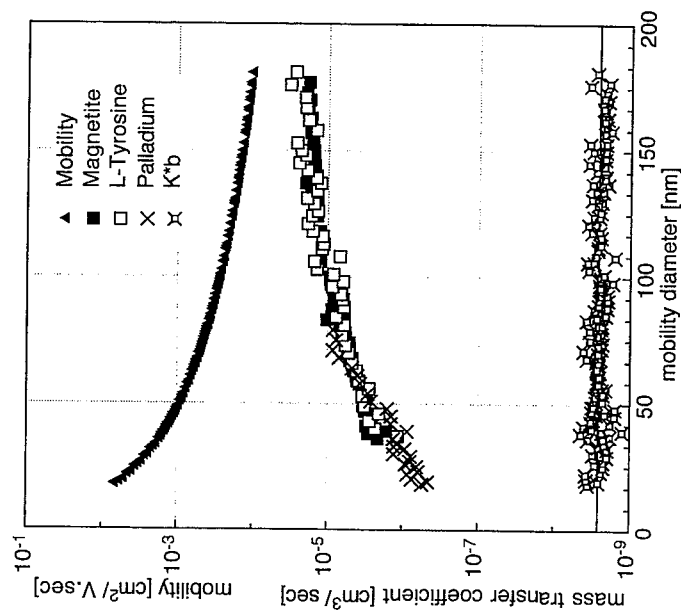


Figure 2. Electrical mobility b , mass transfer coefficient K and Kb for Pd , Fe_3O_4 , and L -Tyrosine particles vs. the mobility diameter. K was determined by attachment of positive air ions to neutral particles.

Fig. 2 shows a similar experiment with a large variety of materials, namely Pd agglomerates which are metallic, spherical particles of magnetite produced in a special oven⁵, and the needle shaped particles forming with the amino acid L -tyrosine⁶. Magnetite (Fe_3O_4) is a poor metal, and L -tyrosine is a dielectric insulator. In this experiment, the attachment coefficient was not determined by radioactive lead, but with the positive air ions produced in a glow discharge. The aerosol was neutralized, and any remaining charged particles were removed in an electrofilter prior to diffusion charging with the positive ions. The ratio of charged aerosol particles N^+ to the uncharged ones, N^+/N_0 , yields the mass transfer coefficient K according to

$$N^+/N_0 = 1 - \exp(-K \cdot t) \quad (6)$$

where t is the appropriately chosen calibration factor of the diffusion charger. It is evident from Fig. 2 that even with these very different particles one obtains $K \cdot b = \text{const}$ within experimental uncertainty over the transition regime. It should be noted that it is really surprising that this holds even for the small mobility diameters. If the image charge played an important role in the diffusion charging, this should show up in: (i) a material dependence of K , (ii) in an upwards curvature of $K \cdot b$ as the mobility diameter decreases. Neither one of these features is observed. However, one must not forget that the full image charge develops only for the dielectric constant $\epsilon \rightarrow \infty$ as realized in electrostatic equilibrium at a plane surface of metals. The ions however fly by the particle in a time $t = \lambda/v \approx 10$ - 10 sec. The dielectric response might be too slow with dielectrics, while metals may possess an oxide layer as well as surface roughness. This can explain the absence of the effects of the electric image charge.

Hence one concludes that $K \cdot b = \text{const}$ is valid independently of particle shape and material, even in the transition regime $dp \approx \lambda$. The simple intuitive understanding of this rule follows from the fact that both, friction $1/b$ and mass transfer K , require collisions with gas molecules.

Only the averaged cross section of the particle determines both b and K . This means that inner surfaces, cracks, roughness and voids do not contribute. Therefore, only a fraction of the geometrical surface is active in collisions with gas phase species. With the larger spherical particles, only a small belt around the equator is actively contributing to friction since only there the relative velocity between gas and particle is high. This fraction of the geometrical surface is the Active Surface. Both the measurement of b or the measurement of K are equivalently suitable to determine the A-surface. b may be obtained in the

differential mobility analyzer (DMA) or in the scanning mobility particle sizer (SMPS). K may be obtained by attachment of radioactive Pb-atoms or simply by diffusion charging of previously neutral particles.

What is the use of knowing b or K or equivalently the A-surface of a particle? It should be noted that the mobility diameter d_p has no physical interpretation. In particular, it is outright wrong to think of πd_p^2 as the relevant surface area of the particle. We know that even with larger spherical particles, it is only a small stripe at the belt of the particle where the relative velocity between particle and gas is high that contributes to the momentum transfer and hence to friction. Similarly, the mass transfer coefficient is only dependent on the diameter of the particle and not on its geometrical surface πd_p^2 with larger particles. The following three cardinal particle properties are determined by b or equivalently by K :

1.) $1/b$ or K measure the Active Surface. It is the fraction of the geometrical surface available for adsorption (or desorption) of gas phase species. The A-surface determines the rate of particle growth by surface condensation, poses the ultimate limit for the speed of chemical reactions, and determines the catalytic activity of the particle.

2.) The diffusion constant is given by $D = kT \cdot b$, hence it is determined by b (kT is the Boltzmann-factor). Deposition of particles in diffusion filters such as the inner respiratory tract is governed by the deposition parameter $\mu = b \cdot kT (L/Q)$, where L is the length of the tube and Q the volume flow rate.

3.) The relaxation time τ of Brownian motion is $\tau = M \cdot b$ where M is the mass of the particle. Deposition of particles by impaction is governed by the stopping distance $\lambda_p = VMb$, V is the velocity of the particle. Therefore, impaction is also determined by b .

Hence we see that from a measurement of b or equivalently K one can evaluate the A-surface and obtain the structural particle properties of concern. The mobility diameter is a highly misleading concept to the non-specialist. In particular, the calculation of particle surfaces or volumes from the mobility diameter will lead to severe errors and contradictions.

The dynamics of the Active Surface

Photoelectric charging is one of the most powerful tools for evaluating the properties of nanoparticles in their natural gaseous environment as it depends on the chemistry and the magnitude of the Active Surface. The gas carrying the particle is irradiated with ultraviolet light. The energy of the photons $h\nu$ must be below the ionization energy of the carrier gas molecules but above the photoelectric threshold Φ of the particles. Under this condition, $h\nu > \Phi$, photoelectrons may be emitted from the surface of the particle into the carrier gas. However, for the emission to occur it is important that the photoelectron is not readsorbed by the particle. One immediately realizes that inner surfaces will not contribute to photoelectric emission of electrons. Similarly, cracks and incisions in the surface can not contribute as the probability is large that the emerging photoelectron hits some other part of its parent particle surface. One is therefore not surprised that the experiments in fact show that the photoelectric yield Y being the probability of electron emission per particle and per incident photon $h\nu$ is proportional to $1/b$, that is to the A-surface.

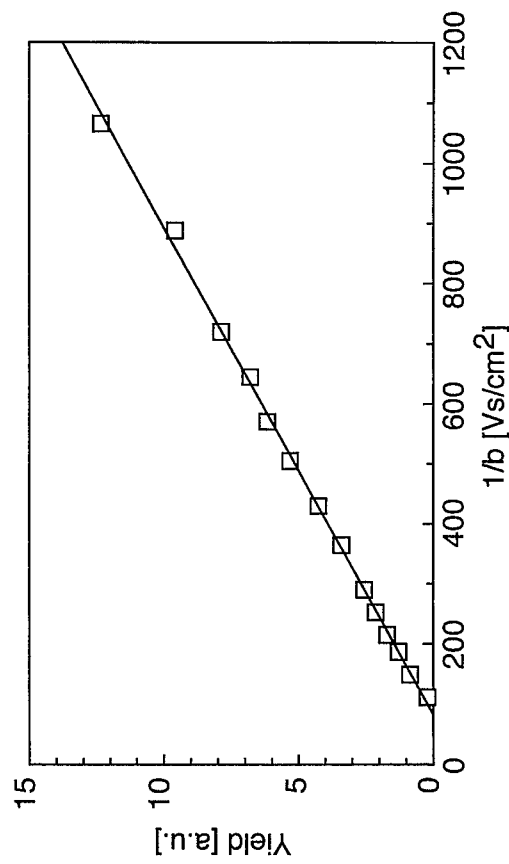


Figure 3. Photoelectric Yield Y vs. the inverse mobility $1/b$ for carbon particles irradiated with ultraviolet light at a wavelength of 183 nm, from Ref. 8.

Fig. 3 shows an experiment on carbon particles from Ref. 8 confirming $Y \propto 1/b$.

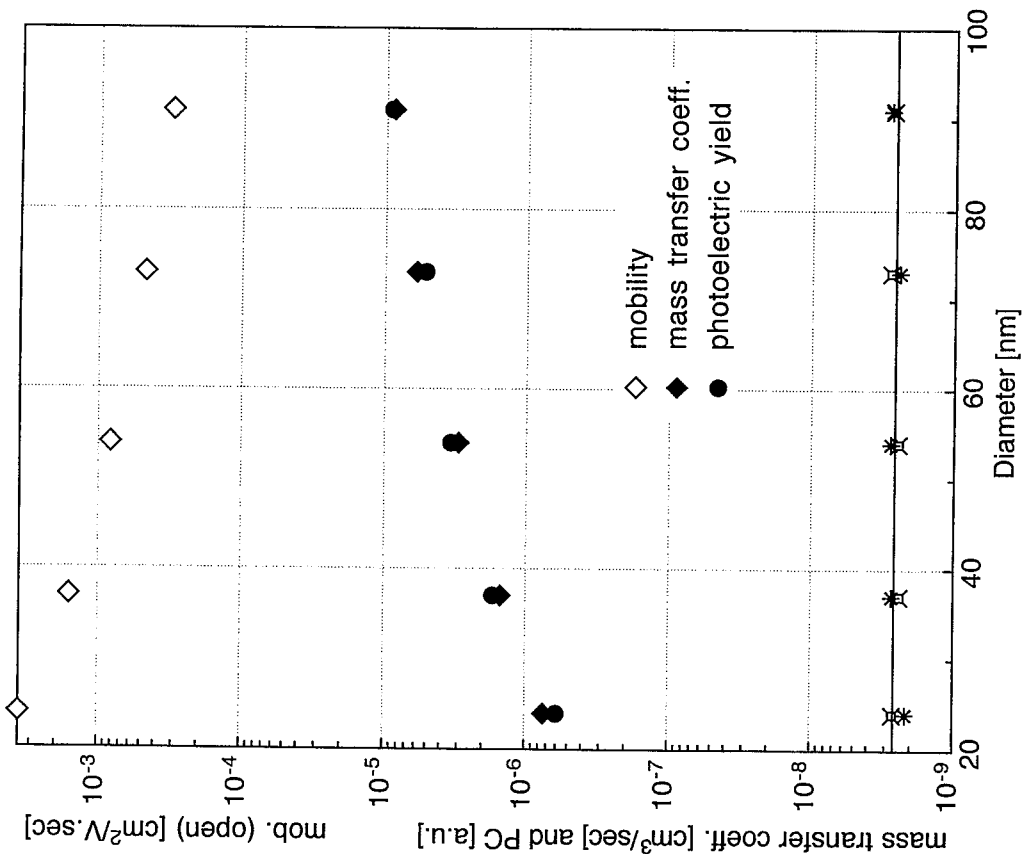


Figure 4. Electrical mobility b , mass transfer coefficient K and photoelectric yield Y vs. the mobility diameter for Ag-agglomerates adapted from Ref. 9. The average value of $Kb = 2.614 \cdot 10^{-9} [cm^5/Vsec^2]$.

Fig. 4 displays the results of an experiment with Ag-agglomerates from Ref. 9 in which the mass transfer coefficient K has been determined by attachment of lead atoms in addition to the measurement of b . It is evident that K as well as the

photoelectric yield Y are proportional to $1/b$, that is $K \cdot b$ or $K \cdot (1/Y)$ are again constant. This appears to be valid even when the mobility diameter is in the range of the mean free path $\lambda = 65$ nm, and even when the particles have bizarre shapes such as occurring with agglomerates.

Hence one finds experimentally that the photoelectric yield measures the same active surface that also determines the other particle properties. The following reasoning can provide some insight.

For large particles with mobility diameters above 200 nm., the onset of classical diffusion leads to back diffusion of the photoelectric charges to the particle.

Filippov et al.⁷ have estimated that the probability p_e of liberation of a photoelectric charge from the particle is given by:

$$p_e = (1 + 3/4 Kn)^{-1} \quad (7)$$

where $Kn = \lambda_e/r_p$ is the Knudsen number, λ_e the mean free path of the photoelectron and $r_p = 1/2 dp$. Eq. (7) shows that $p_e = 1$ for small particles $dp \ll \lambda_e$, but $p_e \rightarrow 0$ when $dp \gg \lambda_e$. The experiment is in agreement with eq. (7) and yields $p_e \approx 0.5$ for $dp = 500$ nm. The photoelectric yield per particle is then $Y = \pi dp^2 \gamma p_e$ where γ is the photoelectric yield per unit surface area. As dp approaches the micrometer range, Y will therefore again increase approximately with dp and not with dp^2 .

As an example for the observation of the dynamics of the active surface we show a measurement of the desorption of perylene $C_{20}H_{12}$ from graphite particles.¹⁰ For this experiment, one needs a pulsed UV-light source such as an excimer laser delivering light pulses of 20 nsec duration. Perylene was chosen as a prototype molecule formed in combustion. This molecule belongs to the family of polycyclic aromatic hydrocarbons (PAH) which contains some extremely carcinogenic species that are linked to the occurrence of lung cancer in humans.

First, one particle mobility is selected in a DMA and then the particles are left in a carrier gas at ambient temperature T_0 in which a partial pressure of perylene is maintained. The perylene adsorbs on the particles until an equilibrium between adsorption and desorption is reached corresponding to the density n_{CH} of perylene in the carrier gas. Subsequently, a small volume of the gas carrying the perylene loaded particles is transported into a hot carrier gas with $n_{CH} = 0$ at the temperature $T > T_0$. Now perylene will start to desorb from the particles. After a given time of the order of 0.1 sec the UV-laser is fired. As the photoelectric yield is much increased when perylene is adsorbed, one can observe the time dependence of the desorption by firing the laser at various delay times after insertion of the

particles into the hot carrier gas, and subsequently measuring the photoelectric charge generated on the particles. Fig. 5 shows the time dependence of the desorption for various temperatures of the carrier gas. One obtains the adsorption enthalpy from these measurements.

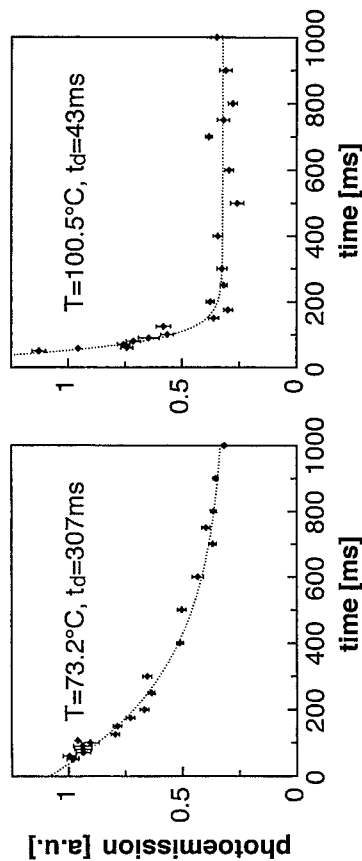


Figure 5. Desorption of perylene from irregular shaped graphitic carbon particles of an average diameter of 25 nm at $T = 72.3\text{ }^{\circ}\text{C}$ and $T = 100.5\text{ }^{\circ}\text{C}$. The dotted lines are exponentials with the time constants t_d indicated fitting the experimental data. From Ref. 10.

Photoelectric charging of nanoparticles has been applied in a number of interesting experiments. It leads to material and surface specific detection of nanoparticles, e.g., of particles generated in combustion¹¹, and more generally to source attribution of combustion aerosols¹². The dynamical changes of the A-surface in catalytic reactions such as occurring in soot reduction by fuel additives has been observed directly¹³. More advanced photoemission experiments employ femtosecond laser pulses to reveal the dynamics of the electrons in nanoparticles and thus give direct access to the electronic structure¹⁴. Nanoparticles built from chiral molecules such as the aminoacids can be selectively detected by employing circularly polarized light for photoelectric charging¹⁵. The alignment of non-spherical particles in an electric field has been observed by the linear dichroism of photoelectric charging¹⁶.

Conclusion

The surface properties of nanoparticles can be evaluated by determining the active surface either by a measurement of the mass transfer coefficient K or equivalently

by a measurement of the mobility b . A simple empirical rule $K \cdot b = \text{const}$ connects the two very different measurements and facilitates the calibration and comparison of different instruments. The dynamics of the active surface are observable in photoelectric charging leading to a detailed understanding of the particle properties and their changes with time in the carrier gas.

References

1. N.A. Fuchs, *The Mechanics of Aerosols*, Dover Publ. Inc., New York 1964
2. W. Fendel et al., *Atmos. Environ.* **29** (1995) 967, and M. Kalberer et al., *J. Phys. Chem.* **100** (1996) 15487
3. A.V. Filippov, *J. Aerosol Sci.* **24** (1993) 423-436
4. S.N. Rogak, U. Baltensperger, and R.C. Flagan, *Aerosol Sci. and Technology* **14** (1991) 447-458
5. A. Keller et al., to be published
6. J. Paul and K. Siegmann, *Chemical Phys. Lett.* **304** (1999) 23-27
7. A.V. Filippov, A. Schmidt-Ott, and W. Fendel, *Aerosol Sci.* **24** (1993), S501-S502
8. H. Burtcher, *J. Aerosol Sci.* **23** (1992) 549-595
9. A. Schmidt-Ott, U. Baltensperger, H.W. Gäggeler, and D.T. Jost, *Aerosol Sci.* **21** (1990) 711-717
10. CH. Hueglin, J. Paul, L. Scherrer, and K. Siegmann, *J. Phys. Chem. B* **101** (1997) 9335-9341
11. U. Matter, H.C. Siegmann, and H. Burtcher, *Environ. Sci. Technol.* **33** (1999) 1946-1952
12. K. Siegmann, L. Scherrer, and H.C. Siegmann, *J. of Molecular Structure (Theochem)* **458** (1999) 191-201
13. M. Kasper et al., *J. Aerosol Sci.* **30** (1999) 217 - 225
14. M. Fierz, K. Siegmann, M. Scharte, and M. Aeschlimann, *Appl. Phys. B* **68** (1999) 415
15. J. Paul, A. Doerzbach, and K. Siegmann, *Phys. Rev. Lett.* **79** (1997) 2947, and Ref. 6
16. A. Keller et al., to be published